

CP violation in multi-body charmless b -hadron decays at LHCb

Adam Morris, on behalf of the LHCb collaboration

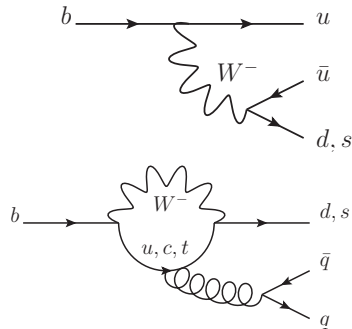
Aix Marseille Univ, CNRS/IN2P3, CPPM

European Physical Society Conference on High Energy Physics
Ghent, 11th July 2019



Charmless b -hadron decays

- Tree $b \rightarrow u$
 - Cabibbo suppression (V_{ub})
- Penguin $b \rightarrow d$ or $b \rightarrow s$
 - Loop-level suppression
 - Sensitive to new particles in the loop
- Similar magnitude of tree & penguin contributions
 - Relative weak phase: interference \rightarrow CP violation
- Rich resonant structure in multi-body decays
 - Strong-phase differences in interference between resonances \rightarrow enhanced CP violation



Charmless three-body B decays

- Rich resonant structure warrants amplitude analysis to measure CP violation in different regions of the phase space
- $B^\pm \rightarrow \pi^\pm \pi^+ \pi^-$ covered in [Jeremy Dalseno's talk](#)
 - LHCb-PAPER-2019-017, LHCb-PAPER-2019-018

This talk:

- Amplitude analysis of $B_s^0 \rightarrow K_S^0 K^\pm \pi^\mp$
 - [JHEP 06 \(2019\) 114](#)
- Amplitude analysis of $B^\pm \rightarrow \pi^\pm K^+ K^-$
 - [arXiv:1905.09244](#)

Charmless four-body b -baryon decays

- CP violation in baryons not yet observed
- Potential for large CP -violating effects in multi-body charmless b -baryon decays

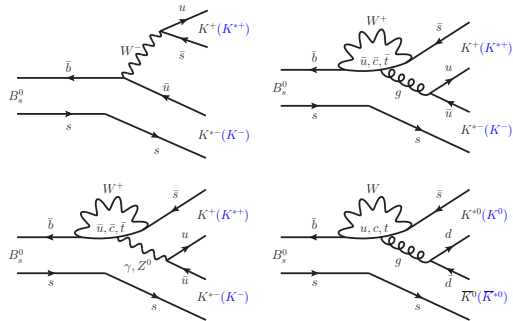
This talk:

- Measurements of $\Delta\mathcal{A}^{CP}$ in charmless four-body Λ_b^0 and Ξ_b decays
 - [arXiv:1903.06792](https://arxiv.org/abs/1903.06792)

$$B_S^0 \rightarrow K_S^0 K^\pm \pi^\mp$$

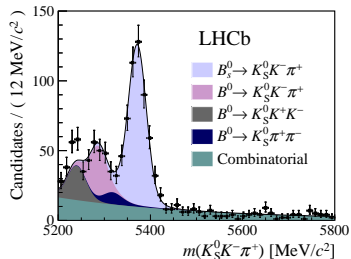
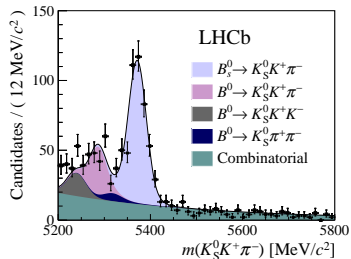
Background

- First observed by LHCb in 1 fb^{-1} from 2011 (JHEP 10 (2013) 143)
- Branching fraction improved in 3 fb^{-1} from 2011+12 (JHEP 11 (2017) 027)
- Specific intermediate states studied
 - $B_s^0 \rightarrow K^{*\pm} K^\mp$ (New J. Phys. 16 (2014) 123001)
 - $B_s^0 \rightarrow K^{*0} K_S^0$ (JHEP 01 (2016) 012)
- Potential for future time-dependent CP violation measurement with larger datasets



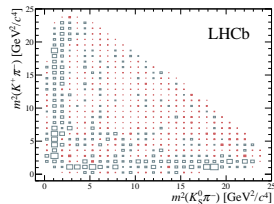
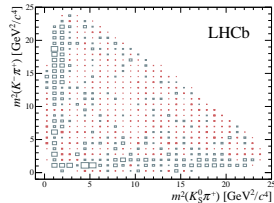
Introduction

- First amplitude analysis of $B_s^0 \rightarrow K_S^0 K^\pm \pi^\mp$
 - Untagged and time-integrated
 - Simultaneous amplitude fit of two final states
 - Novel approach
- 431 $B_s^{0(-)} \rightarrow K_S^0 K^+ \pi^- + 489 B_s^{0(-)} \rightarrow K_S^0 K^- \pi^+$
- Run 1 dataset: 3 fb^{-1} from 2011+12
- Published as [JHEP 06 \(2019\) 114](#)



Amplitude model

- Both B_s^0 and \bar{B}_s^0 can decay to each final state, although not necessarily with the same amplitude $A_f \neq \bar{A}_f$
- Untagged analysis means B_s^0 and \bar{B}_s^0 cannot be distinguished
- Fit for effective amplitude that is a combination of A_f and \bar{A}_f
- $K^+ K_S^0$ resonances e.g. $a_2(1320)^+$ considered but not seen in fit
- $K\pi$ P-wave and D-wave modelled with Breit–Wigners
- $K\pi$ S-wave modelled with the LASS lineshape
 - Combines $K_0^*(1430)$ and non-resonant $K\pi$
 - Possible to disentangle later when calculating $\mathcal{B}(B_s^0 \rightarrow K_0^*(1430)K)$

 $K_S^0 K^+ \pi^-$

 $K_S^0 K^- \pi^+$


Fit results

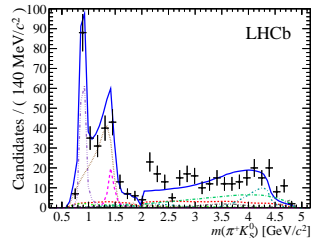
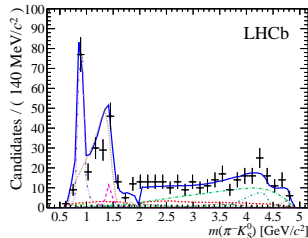
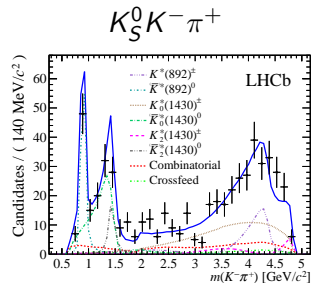
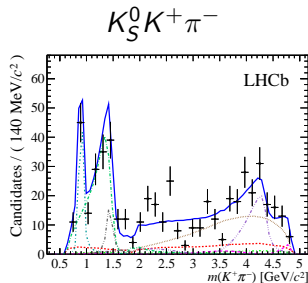
$K_S^0 K^+ \pi^-$		$K_S^0 K^- \pi^+$	
Resonance	Frac. (%)	Resonance	Frac. (%)
$K^*(892)^-$	15.6 ± 1.5	$K^*(892)^+$	13.4 ± 2.0
$K_0^*(1430)^-$	30.2 ± 2.6	$K_0^*(1430)^+$	28.5 ± 3.6
$K_2^*(1430)^-$	2.9 ± 1.3	$K_2^*(1430)^+$	5.8 ± 1.9
$K^*(892)^0$	13.2 ± 2.4	$\bar{K}^*(892)^0$	19.2 ± 2.3
$K_0^*(1430)^0$	33.9 ± 2.9	$\bar{K}_0^*(1430)^0$	27.0 ± 4.1
$K_2^*(1430)^0$	5.9 ± 4.0	$\bar{K}_2^*(1430)^0$	7.7 ± 2.8

NB: uncertainties are statistical only

- Fit fractions for each resonance and its conjugate are consistent, hence no significant CP violation observed

Sources of systematics:

- Mismodelling in mass fit
- Efficiency and background models
- Fit bias
- Fixed parameters
- Amplitude model



Branching fractions

Flavour-averaged fit fractions converted to branching fractions for the quasi-two-body modes

First observations of $B_s^0 \rightarrow K_0^*(1430)K$ modes

$$\mathcal{B}(B_s^0 \rightarrow K^*(892)^\pm K^\mp) = (18.6 \pm 1.2 \pm 0.8 \pm 4.0 \pm 2.0) \times 10^{-6}$$

$$\mathcal{B}(B_s^0 \rightarrow K_0^*(1430)^\pm K^\mp) = (31.3 \pm 2.3 \pm 0.7 \pm 25.1 \pm 3.3) \times 10^{-6}$$

$$\mathcal{B}(B_s^0 \rightarrow K_2^*(1430)^\pm K^\mp) = (10.3 \pm 2.5 \pm 1.1 \pm 16.3 \pm 1.1) \times 10^{-6}$$

$$\mathcal{B}(B_s^0 \rightarrow \overleftarrow{K}^*(892)^0 \overleftarrow{K}^0) = (19.8 \pm 2.8 \pm 1.2 \pm 4.4 \pm 2.1) \times 10^{-6}$$

$$\mathcal{B}(B_s^0 \rightarrow \overleftarrow{K}_0^*(1430)^0 \overleftarrow{K}^0) = (33.0 \pm 2.5 \pm 0.9 \pm 9.1 \pm 3.5) \times 10^{-6}$$

$$\mathcal{B}(B_s^0 \rightarrow \overleftarrow{K}_2^*(1430)^0 \overleftarrow{K}^0) = (16.8 \pm 4.5 \pm 1.7 \pm 21.2 \pm 1.8) \times 10^{-6}$$

Uncertainties: \pm stat \pm syst \pm model \pm norm

“norm” refers to uncertainty on $\mathcal{B}(B_s^0 \rightarrow K^0 K^\pm \pi^\mp)$

Branching fractions

Branching fractions of non-resonant modes:

$$\mathcal{B}(B_s^0 \rightarrow (\overline{K}^0 \pi^\pm)_{\text{NR}} K^\mp) = (11.4 \pm 0.8 \pm 0.2 \pm 9.2 \pm 1.2 \pm 0.5) \times 10^{-6}$$

$$\mathcal{B}(B_s^0 \rightarrow (K^\mp \pi^\pm)_{\text{NR}} \overline{K}^0) = (12.1 \pm 0.9 \pm 0.3 \pm 3.3 \pm 1.3 \pm 0.5) \times 10^{-6}$$

Uncertainties: \pm stat \pm syst \pm model \pm norm \pm eff. range

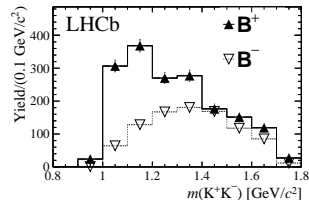
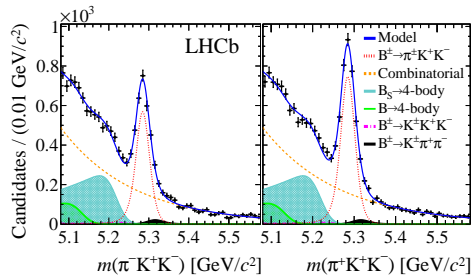
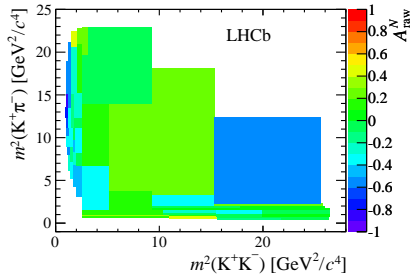
Fifth uncertainty related to proportion of the $(K\pi)_0^*$ component due to the effective range part of the LASS lineshape.

$$B^\pm \rightarrow \pi^\pm K^+ K^-$$

Background

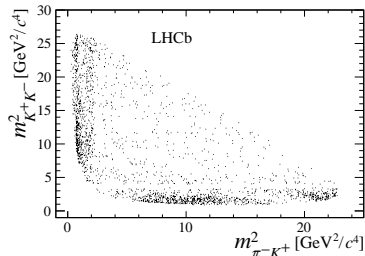
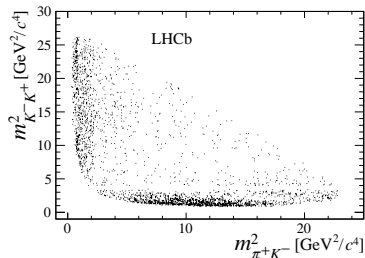
Previously studied by LHCb
(Phys. Rev. D 90 (2014) 112004)

- Binned model-independent analysis
- Total $\mathcal{A}^{CP} = -0.123 \pm 0.017 \pm 0.012 \pm 0.007$
- Regions of phase space with much larger \mathcal{A}^{CP}



Introduction

- First amplitude analysis of $B^\pm \rightarrow \pi^\pm K^+ K^-$
 - $\pi^\pm K^\mp$ resonances: $K^*(892)^0$, $K_0^*(1430)^0$
 - Single-pole form factor to describe non-resonant $\pi^\pm K^\mp$
 - $K^+ K^-$ resonances: $\phi(1020)$, $f_2(1270)$, $\rho(1450)^0$
 - Dedicated $\pi\pi \leftrightarrow KK$ rescattering amplitude
- Run 1 dataset: 3 fb^{-1} from 2011+12
- Candidates in signal region: 2052 B^+ , 1566 B^-
- Submitted to PRL



Non-resonant single-pole form factor

Proposed by Alvarenga Nogueira *et al.* (*Phys. Rev. D* 92 (2015) 054010)

$$\mathcal{A}_{\text{source}} = \left(1 + \frac{s}{\Lambda^2}\right)^{-1}$$

- $s = m_{\pi^\pm K^\mp}^2$
- $\Lambda = 1 \text{ GeV}/c^2$ sets the scale for the energy dependence

$\pi\pi \leftrightarrow KK$ rescattering amplitude

Based on Pelaez and Yndurain (Phys. Rev. D 71 (2005) 074016)

$$\mathcal{A}_{\text{rescattering}} = \left(1 + \frac{s}{\Lambda^2}\right)^{-1} \sqrt{1 - \nu^2} e^{2i\delta}$$

Inelasticity, ν :

$$\nu = 1 - \left(\epsilon_1 \frac{k_2}{\sqrt{s}} + \epsilon_2 \frac{k_2^2}{s} \right) \frac{M'^2 - s}{s}$$

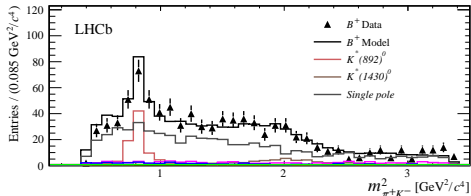
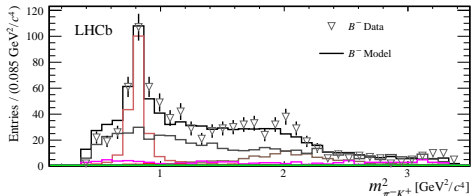
Phase shift δ :

$$\cot \delta = C_0 \frac{(s - M_s^2)(M_f^2 - s)}{M_f^2 \sqrt{s}} \frac{|k_2|}{k_2^2}$$

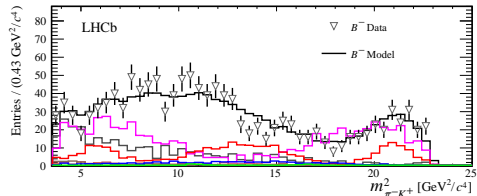
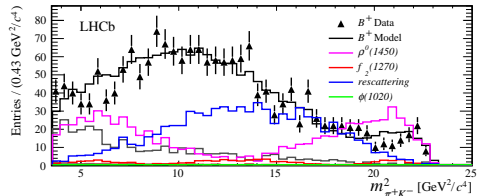
- $s = m_{K^+K^-}^2$
- $k_2 = \frac{1}{2} \sqrt{2 - 4m_K}$
 - $m_K = 0.495 \text{ GeV}/c^2$
- $M' = 1.5 \text{ GeV}/c^2$
- $M_s = 0.92 \text{ GeV}/c^2$
- $M_f = 1.32 \text{ GeV}/c^2$
- $\epsilon_1 = 2.4$
- $\epsilon_2 = -5.5$
- $C_0 = 1.3$

The $\pi^\pm K^\mp$ spectrum

$$m_{\pi^\pm K^\mp}^2 < 3.5 \text{ GeV}^2/c^4$$

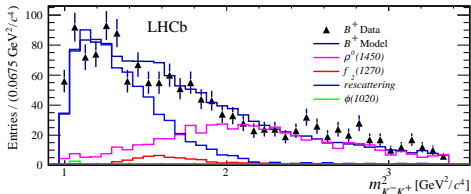
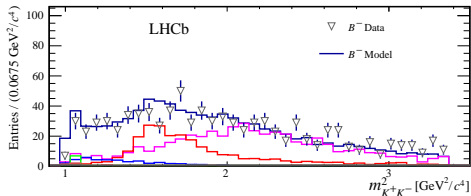
 B^+  B^- 

$$m_{\pi^\pm K^\mp}^2 > 3.5 \text{ GeV}^2/c^4$$



- Single-pole non-resonant is dominant contribution ($\sim 32\%$)
- $\rho(1450)^0 - f_2(1270)$ destructive interference at high $m_{\pi^\pm K^\mp}^2$

The K^+K^- spectrum

 B^+  B^- 

- $\rho(1450)^0 \sim 30\%$ contribution
 - Unexpectedly large for K^+K^-
 - Further analysis with more data needed
- $\pi\pi \leftrightarrow KK \sim 16\%$ contribution
 - Large CP asymmetry

Results

Contribution	Fit Fraction(%)	$\mathcal{A}^{CP}(\%)$
$K^*(892)^0$	$7.5 \pm 0.6 \pm 0.5$	$+12.3 \pm 8.7 \pm 4.5$
$K_0^*(1430)^0$	$4.5 \pm 0.7 \pm 1.2$	$+10.4 \pm 14.9 \pm 8.8$
Single pole	$32.3 \pm 1.5 \pm 4.1$	$-10.7 \pm 5.3 \pm 3.5$
$\rho(1450)^0$	$30.7 \pm 1.2 \pm 0.9$	$-10.9 \pm 4.4 \pm 2.4$
$f_2(1270)$	$7.5 \pm 0.8 \pm 0.7$	$+26.7 \pm 10.2 \pm 4.8$
Rescattering	$16.4 \pm 0.8 \pm 1.0$	$-66.4 \pm 3.8 \pm 1.9$
$\phi(1020)$	$0.3 \pm 0.1 \pm 0.1$	$+9.8 \pm 43.6 \pm 26.6$

Sources of systematics:

- Mismodelling in mass fit
- Efficiency and background models
- Fit bias
- Fixed parameters

- $\pi\pi \leftrightarrow KK$ rescattering: largest ever CP asymmetry for a single amplitude to date
- No significant CP asymmetry observed in the other components
- $\phi(1020)$ contribution not significant

Four-body Λ_b^0 and Ξ_b^0 decays

Background

Previous LHCb results on charmless four-body b -baryon decays:

- Branching fractions ([JHEP 02 \(2018\) 098](#))
- Triple-product asymmetries: ([Nature Phys. 13 \(2017\) 391-396](#), [JHEP 08 \(2018\) 039](#))
- 3.3σ evidence for CP violation in $\Lambda_b^0 \rightarrow p\pi^-\pi^+\pi^-$ from triple-products

Introduction

- \mathcal{A}^{CP} using Λ_b^0/Ξ_b^0 and $\bar{\Lambda}_b^0/\bar{\Xi}_b^0$ yields obtained from fitting $m(phh'h'')$

$$\mathcal{A}^{CP} \equiv \frac{\Gamma(X_b^0 \rightarrow f) - \Gamma(\bar{X}_b^0 \rightarrow \bar{f})}{\Gamma(X_b^0 \rightarrow f) + \Gamma(\bar{X}_b^0 \rightarrow \bar{f})}$$

- Complementary to triple-products
- Run 1 dataset: 3 fb^{-1} from 2011+12
- Submitted to EPJC

- Six decay modes studied:

- $\Lambda_b^0 \rightarrow p\pi^-\pi^+\pi^-$
- $\Lambda_b^0 \rightarrow pK^-\pi^+\pi^-$
- $\Lambda_b^0 \rightarrow pK^-K^+\pi^-$
- $\Lambda_b^0 \rightarrow pK^-K^+K^-$
- $\Xi_b^0 \rightarrow pK^-\pi^+\pi^-$
- $\Xi_b^0 \rightarrow pK^-\pi^+K^-$

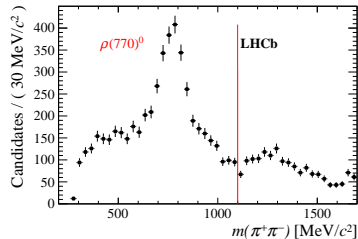
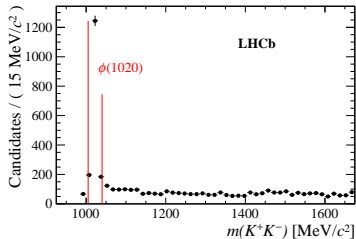
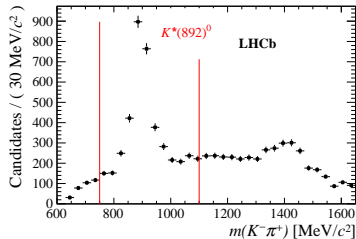
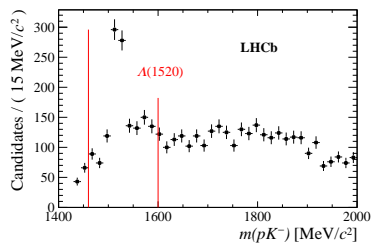
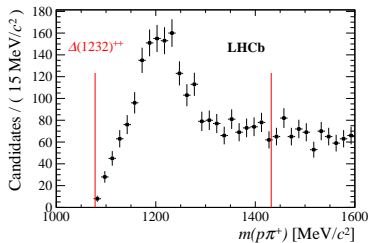
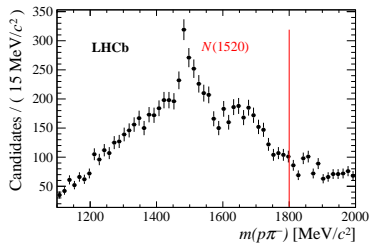
- For the **three most abundant decays**, also study specific regions of phase space

- Low two-body mass
- Specific intermediate resonances

- $\Lambda_b^0 \rightarrow \Lambda_c^+\pi^-$ and $\Xi_b^0 \rightarrow \Xi_c^+\pi^-$ control channels to cancel production and detection asymmetries

- $\Delta\mathcal{A}^{CP} = \mathcal{A}_{\text{charmless}}^{CP} - \mathcal{A}_{\text{charm}}^{CP}$

Phase space regions



Mass fits

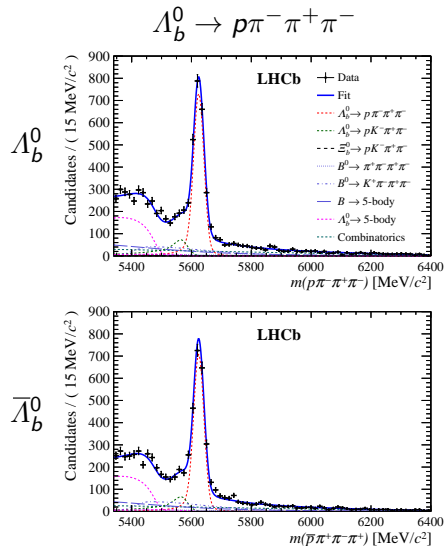
Simultaneous maximum likelihood fit to b -hadron candidates under each $phh'h''$ hypothesis

Data split by:

- Proton charge
- Year of data-taking
- Hardware trigger condition

Fit model has components for:

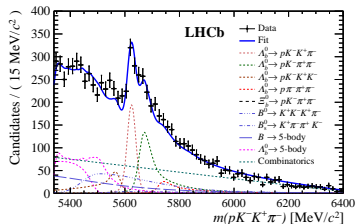
- Signal
- Cross-feed ($\pi - K$ mis-ID)
- 4-body B -meson decays ($p - \pi$ and $p - K$ mis-ID)
- 5-body b -hadron decays
- Combinatorial background



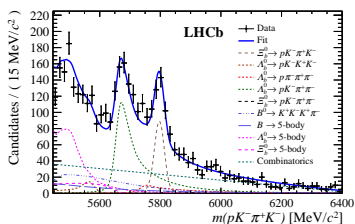
Sample fit projections

$$\Lambda_b^0 \rightarrow pK^-K^+\pi^-$$

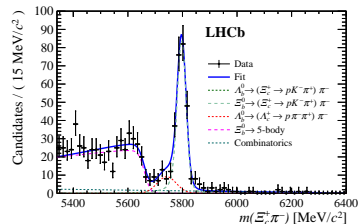
X_b



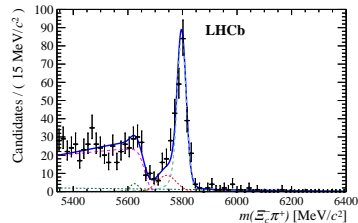
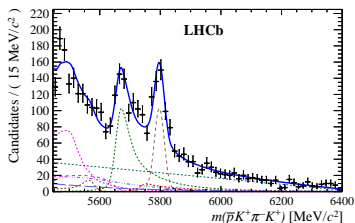
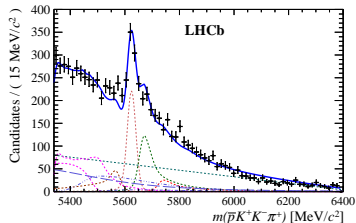
$$\Xi_b^0 \rightarrow pK^-\pi^+K^-$$



$$\Xi_b^0 \rightarrow (\Xi_c^+ \rightarrow pK^-\pi^+)\pi^-$$

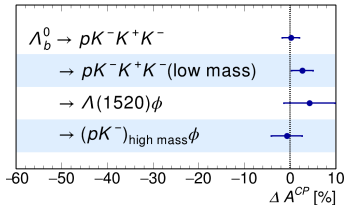
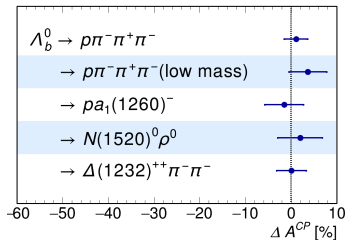
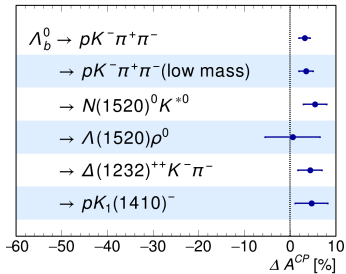
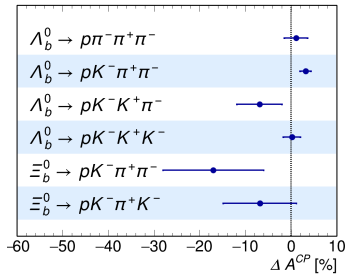


\bar{X}_b



Results

- Total of 18 $\Delta\mathcal{A}^{CP}$ measurements
- No indication of significant CPV
- Statistical uncertainty dominates
- $\sim 5\times$ larger yields in Run 2 data



Summary and conclusions

Summary

$$B_s^0 \rightarrow K_S^0 K^\pm \pi^\mp$$

- No evidence of CP violation
- Updated quasi-two-body branching fractions
- First observation of $B_s^0 \rightarrow K_0^*(1430)K$ modes

$$B^\pm \rightarrow \pi^\pm K^+ K^-$$

- $\mathcal{A}^{CP} = (-66.4 \pm 4.2)\%$ in $\pi\pi \leftrightarrow KK$ rescattering term
- Largest CP asymmetry in a single amplitude

Four-body b -baryon decays

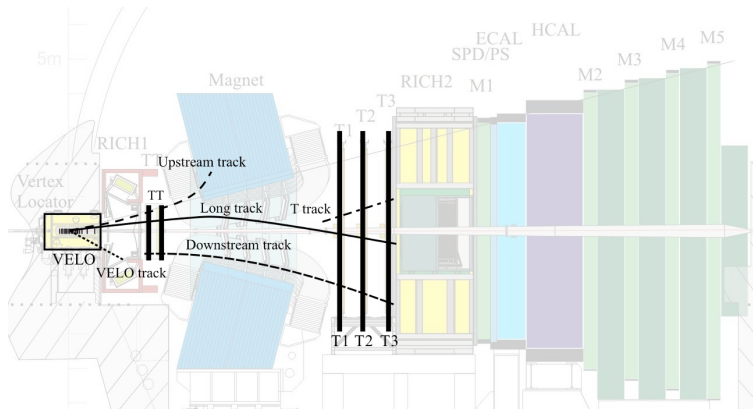
- 18 $\Delta\mathcal{A}^{CP}$ measurements
- No evidence of CP violation

Conclusions

- Multi-body charmless b -hadron decays are an important area for studying CP violation
- LHCb Run 2 data and upgrade will provide improved results

Backup slides

Track types at LHCb



- Long tracks pass through all tracking stations
- Downstream tracks pass through the TT and T
 - Λ and K_S^0 can decay outside VELO

Run 1 performance paper:
LHCb-DP-2014-002

$$B_S^0 \rightarrow K_S^0 K^\pm \pi^\mp$$

B_s^0 mass fit

- Simultaneous fit to $m(K_S^0 K^\pm \pi^\mp)$ in 24 data categories:
 - 3 data-taking periods (change in trigger efficiency during 2012)
 - 4 final states (including $\pi \leftrightarrow K$ mis-ID)
 - 2 K_S^0 reconstruction categories: decay inside (“long”) or outside (“downstream”) VELO
- Signal and cross-feed: sum of two Crystal Ball functions
- Combinatorial background: exponential function

B_s^0 mass fit

Final state	K_S^0 category	Sample	B_s^0 signal		Combinatorial		Cross-feed	
			Full range	2.5σ	Full range	2.5σ	Full range	2.5σ
$K_S^0 K^+ \pi^-$	downstream	2011	73.6 ± 10.6	72.1	108.3 ± 15.1	22.1	8.9 ± 2.8	1.7
		2012a	48.2 ± 8.6	45.7	70.1 ± 12.1	14.3	7.3 ± 3.8	1.1
		2012b	135.3 ± 13.6	130.0	87.4 ± 13.8	17.9	17.0 ± 5.6	3.1
	long	2011	76.2 ± 9.8	74.6	44.1 ± 9.8	8.4	8.2 ± 1.7	1.8
		2012a	38.5 ± 7.7	36.8	58.8 ± 11.2	11.2	7.8 ± 1.8	0.9
		2012b	73.5 ± 10.6	71.9	71.7 ± 13.1	13.6	15.9 ± 2.5	1.7
total			431.1		87.5		10.3	
$K_S^0 K^- \pi^+$	downstream	2011	72.8 ± 10.3	71.4	78.9 ± 12.7	16.1	8.2 ± 2.4	1.3
		2012a	68.8 ± 9.6	65.2	46.2 ± 9.9	9.5	7.0 ± 3.4	1.2
		2012b	165.1 ± 15.2	158.6	104.1 ± 15.0	21.3	17.3 ± 5.8	2.9
	long	2011	77.3 ± 9.8	75.7	39.0 ± 10.2	7.4	9.6 ± 1.7	1.4
		2012a	40.3 ± 8.1	38.5	58.9 ± 11.9	11.2	8.6 ± 1.8	0.7
		2012b	81.7 ± 10.4	80.0	50.1 ± 12.3	9.5	15.0 ± 2.5	1.4
total			489.4		75.0		8.9	

Systematics

Resonance	Yields	Bkg.	Eff.	Fit fraction (%) uncertainties					Total
				Fit bias	Add. res.	Fixed par.	Alt. model	Method	
$K^*(892)^-$	0.2	0.2	0.5	0.2	–	0.7	5.4	3.1	6.3
$K_0^*(1430)^-$	0.1	0.2	0.6	0.3	0.1	2.1	22.0	2.9	22.3
$K_2^*(1430)^-$	0.1	0.1	0.3	0.6	0.1	1.8	2.2	0.2	2.9
$K^*(892)^0$	0.2	0.2	0.4	0.9	–	0.3	7.0	2.0	7.4
$K_0^*(1430)^0$	0.2	0.3	0.9	0.4	0.1	4.4	3.3	1.3	5.7
$K_2^*(1430)^0$	0.1	0.3	0.7	1.3	0.2	4.4	3.6	1.0	6.0
$K^*(892)^+$	0.4	0.1	0.6	0.5	0.1	0.7	1.1	0.7	1.8
$K_0^*(1430)^+$	0.5	0.4	0.7	0.8	0.2	6.4	13.0	4.5	15.2
$K_2^*(1430)^+$	0.1	0.2	0.4	0.2	0.1	4.1	4.5	3.2	6.9
$\bar{K}^*(892)^0$	0.4	0.3	0.4	0.2	0.2	0.5	3.0	7.9	8.5
$\bar{K}_0^*(1430)^0$	0.4	0.4	0.6	0.8	0.7	0.9	3.9	5.4	6.8
$\bar{K}_2^*(1430)^0$	0.1	0.2	0.4	0.8	0.1	1.0	5.5	2.7	6.3

$$B^\pm \rightarrow \pi^\pm K^+ K^-$$

B-factory results on $B^\pm \rightarrow \pi^\pm K^+ K^-$

LHCb \mathcal{A}^{CP} results (reminder):

- Total \mathcal{A}^{CP} : $-0.123 \pm 0.017 \pm 0.012 \pm 0.007$
(Phys. Rev. D 90 (2014) 112004)
- $\pi\pi \leftrightarrow KK$ \mathcal{A}^{CP} : $-66.4 \pm 3.8 \pm 1.9$
(arXiv:1905.09244)

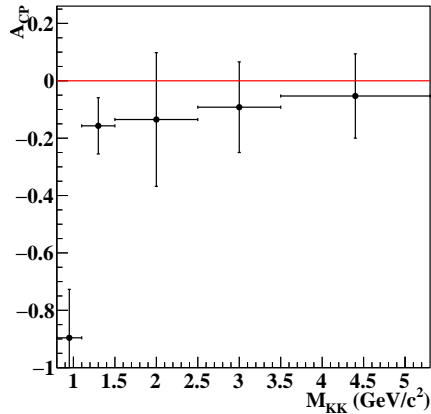
Belle \mathcal{A}^{CP} results:

- Total \mathcal{A}^{CP} : $-0.170 \pm 0.073 \pm 0.017$
(Phys. Rev. D 96 (2017) 031101)

Branching fractions:

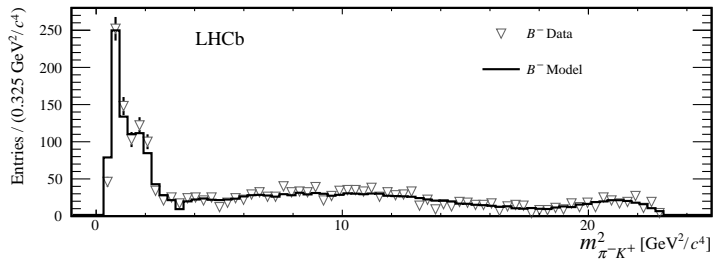
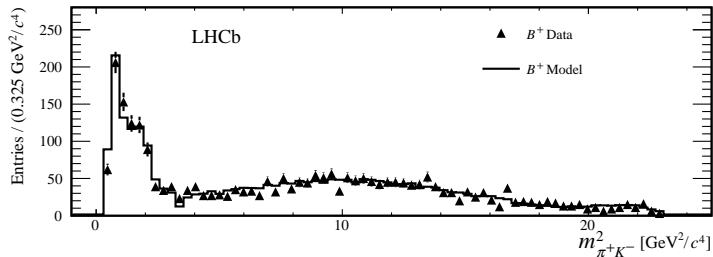
- Belle: $(5.38 \pm 0.40 \pm 0.35) \times 10^{-6}$
(Phys. Rev. D 96 (2017) 031101)
- BaBar: $(5.0 \pm 0.5 \pm 0.5) \times 10^{-6}$
(Phys. Rev. Lett. 99 (2007) 221801)

Belle \mathcal{A}^{CP} in bins of $m(K^+ K^-)$

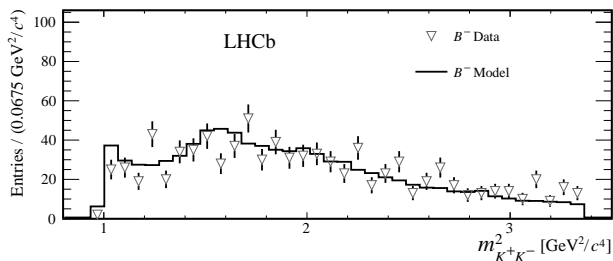
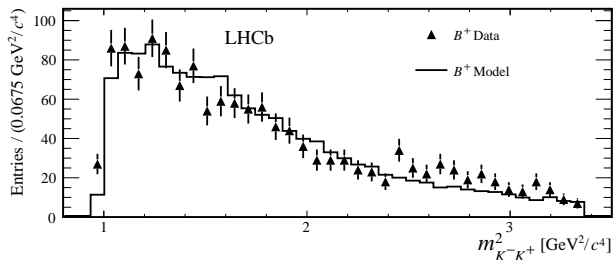


(Phys. Rev. D 96 (2017) 031101)

Projections



Projections



Results

Contribution	Fit Fraction(%)	$\mathcal{A}^{CP}(\%)$	Magnitude (B^+/B^-)	Phase[$^\circ$] (B^+/B^-)
$K^*(892)^0$	$7.5 \pm 0.6 \pm 0.5$	$+12.3 \pm 8.7 \pm 4.5$	$0.94 \pm 0.04 \pm 0.02$	0 (fixed)
			$1.06 \pm 0.04 \pm 0.02$	0 (fixed)
$K_0^*(1430)^0$	$4.5 \pm 0.7 \pm 1.2$	$+10.4 \pm 14.9 \pm 8.8$	$0.74 \pm 0.09 \pm 0.09$	$-176 \pm 10 \pm 16$
			$0.82 \pm 0.09 \pm 0.10$	$136 \pm 11 \pm 21$
Single pole	$32.3 \pm 1.5 \pm 4.1$	$-10.7 \pm 5.3 \pm 3.5$	$2.19 \pm 0.13 \pm 0.17$	$-138 \pm 7 \pm 5$
			$1.97 \pm 0.12 \pm 0.20$	$166 \pm 6 \pm 5$
$\rho(1450)^0$	$30.7 \pm 1.2 \pm 0.9$	$-10.9 \pm 4.4 \pm 2.4$	$2.14 \pm 0.11 \pm 0.07$	$-175 \pm 10 \pm 15$
			$1.92 \pm 0.10 \pm 0.07$	$140 \pm 13 \pm 20$
$f_2(1270)$	$7.5 \pm 0.8 \pm 0.7$	$+26.7 \pm 10.2 \pm 4.8$	$0.86 \pm 0.09 \pm 0.07$	$-106 \pm 11 \pm 10$
			$1.13 \pm 0.08 \pm 0.05$	$-128 \pm 11 \pm 14$
Rescattering	$16.4 \pm 0.8 \pm 1.0$	$-66.4 \pm 3.8 \pm 1.9$	$1.91 \pm 0.09 \pm 0.06$	$-56 \pm 12 \pm 18$
			$0.86 \pm 0.07 \pm 0.04$	$-81 \pm 14 \pm 15$
$\phi(1020)$	$0.3 \pm 0.1 \pm 0.1$	$+9.8 \pm 43.6 \pm 26.6$	$0.20 \pm 0.07 \pm 0.02$	$-52 \pm 23 \pm 32$
			$0.22 \pm 0.06 \pm 0.04$	$107 \pm 33 \pm 41$

Four-body Λ_b^0 and Ξ_b^0 decays

Triple-product asymmetries in $\Lambda_b^0 \rightarrow p\pi^-\pi^+\pi^-$

$$C_{\hat{T}} = \vec{p}_p \cdot (\vec{p}_{h_1^-} \times \vec{p}_{h_2^+}) \text{ for } \Lambda_b^0$$

$$\bar{C}_{\hat{T}} = \vec{p}_{\bar{p}} \cdot (\vec{p}_{h_1^+} \times \vec{p}_{h_2^-}) \text{ for } \bar{\Lambda}_b^0$$

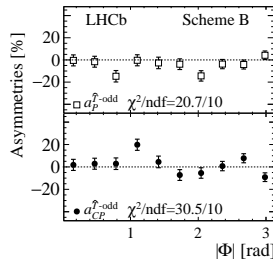
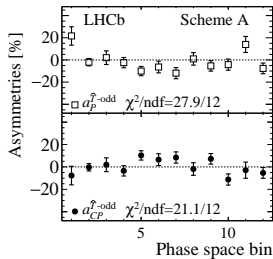
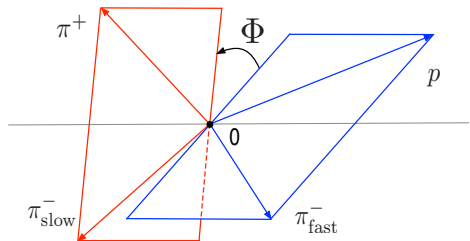
$$A_{\hat{T}}(C_{\hat{T}}) = \frac{N(C_{\hat{T}} > 0) - N(C_{\hat{T}} < 0)}{N(C_{\hat{T}} > 0) + N(C_{\hat{T}} < 0)}$$

$$\bar{A}_{\hat{T}}(\bar{C}_{\hat{T}}) = \frac{\bar{N}(-\bar{C}_{\hat{T}} > 0) - \bar{N}(-\bar{C}_{\hat{T}} < 0)}{\bar{N}(-\bar{C}_{\hat{T}} > 0) + \bar{N}(-\bar{C}_{\hat{T}} < 0)}$$

The P - and CP -violating observables are defined as

$$a_P^{\hat{T}\text{-odd}} = \frac{1}{2} (A_{\hat{T}} + \bar{A}_{\hat{T}})$$

$$a_{CP}^{\hat{T}\text{-odd}} = \frac{1}{2} (A_{\hat{T}} - \bar{A}_{\hat{T}})$$



Control channels

The difference of CP -asymmetries measured for the charmless modes and for the control channels results in $\Delta\mathcal{A}^{CP}$ measurements. For each observable, the choice of the control channel is aiming at cancelling at first order production and detection asymmetries.

Charmless mode	Control channel
$\Lambda_b^0 \rightarrow p\pi^-\pi^+\pi^-$	$\Lambda_b^0 \rightarrow (\Lambda_c^+ \rightarrow p\pi^-\pi^+)\pi^-$
$\Lambda_b^0 \rightarrow pK^-\pi^+\pi^-$	$\Lambda_b^0 \rightarrow (\Lambda_c^+ \rightarrow pK^-\pi^+)\pi^-$
$\Lambda_b^0 \rightarrow pK^-K^+\pi^-$	$\Lambda_b^0 \rightarrow (\Lambda_c^+ \rightarrow p\pi^-\pi^+)\pi^-$
$\Lambda_b^0 \rightarrow pK^-K^+K^-$	$\Lambda_b^0 \rightarrow (\Lambda_c^+ \rightarrow pK^-\pi^+)\pi^-$
$\Xi_b^0 \rightarrow pK^-\pi^+\pi^-$	$\Xi_b^0 \rightarrow (\Xi_c^+ \rightarrow pK^-\pi^+)\pi^-$
$\Xi_b^0 \rightarrow pK^-\pi^+K^-$	$\Xi_b^0 \rightarrow (\Xi_c^+ \rightarrow pK^-\pi^+)\pi^-$

Phase space regions

Decay mode	Invariant-mass requirements (in MeV/c^2)
$\Lambda_b^0 \rightarrow p\pi^-\pi^+\pi^-$ low mass	$m(p\pi^-) < 2000$ and $m(\pi^+\pi^-) < 1640$
$\Lambda_b^0 \rightarrow pa_1(1260)^-$	$419 < m(\pi^+\pi^-\pi^+) < 1500$
$\Lambda_b^0 \rightarrow N(1520)^0\rho^0$	$1078 < m(p\pi^-) < 1800$ and $m(\pi^+\pi^-) < 1100$
$\Lambda_b^0 \rightarrow \Delta(1232)^{++}\pi^-\pi^-$	$1078 < m(p\pi^+) < 1432$

Phase space regions

Decay mode	Invariant-mass requirements (in MeV/c^2)
$\Lambda_b^0 \rightarrow pK^-\pi^+\pi^-$ low mass	$m(pK^-) < 2000$ and $m(\pi^+\pi^-) < 1640$
$\Lambda_b^0 \rightarrow N(1520)^0 K^{*0}$	$1078 < m(p\pi^-) < 1800$ and $750 < m(\pi^+K^-) < 1100$
$\Lambda_b^0 \rightarrow \Lambda(1520)\rho^0$	$1460 < m(pK^-) < 1580$ and $m(\pi^+\pi^-) < 1100$
$\Lambda_b^0 \rightarrow \Delta(1232)^{++} K^-\pi^-$	$1078 < m(p\pi^+) < 1432$
$\Lambda_b^0 \rightarrow pK_1(1410)^-$	$1200 < m(K^-\pi^+\pi^-) < 1600$

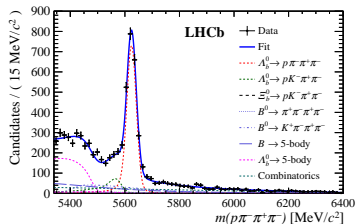
Phase space regions

Decay mode	Invariant-mass requirements (in MeV/c^2)
$\Lambda_b^0 \rightarrow pK^- K^+ K^-$ low mass	$m(pK^-) < 2000$ and $m(K^+ K^-) < 1675$
$\Lambda_b^0 \rightarrow \Lambda(1520)\phi$	$1460 < m(pK^-) < 1600$ and $1005 < m(K^+ K^-) < 1040$
$\Lambda_b^0 \rightarrow (pK^-)_{\text{high-mass}}\phi$	$m(pK^-) > 1600$ and $1005 < m(K^+ K^-) < 1040$

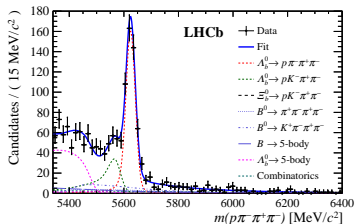
Fit projections

 X_b

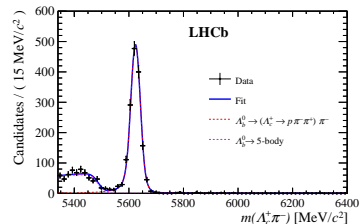
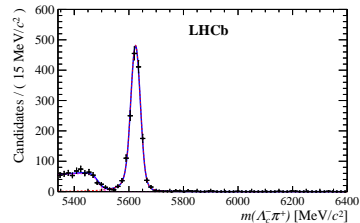
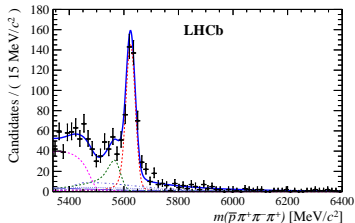
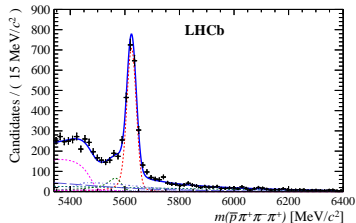
$$\Lambda_b^0 \rightarrow p\pi^-\pi^+\pi^-$$



$$\Lambda_b^0 \rightarrow p\pi^-\pi^+\pi^- \text{ low mass}$$

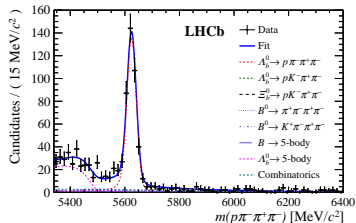


$$\Lambda_b^0 \rightarrow (\Lambda_c^+ \rightarrow p\pi^-\pi^+)\pi^-$$

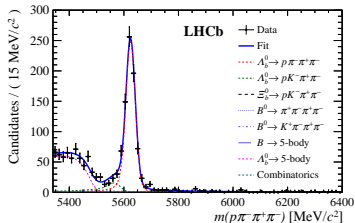
 \bar{X}_b 

Fit projections

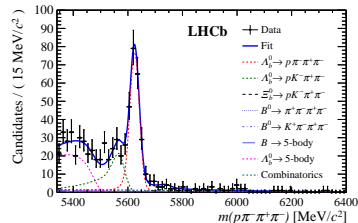
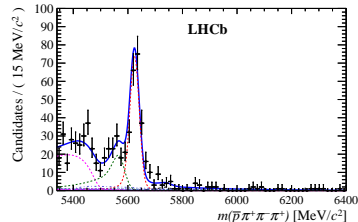
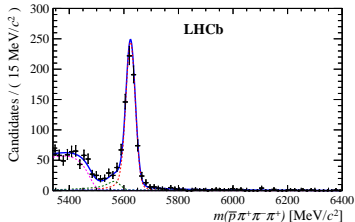
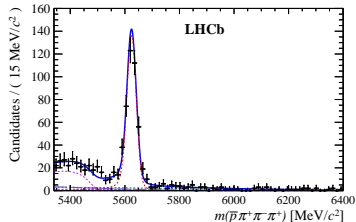
$$\Lambda_b^0 \rightarrow p a_1(1260)^-$$

 X_b


$$\Lambda_b^0 \rightarrow \Delta(1232)^{++} \pi^- \pi^-$$



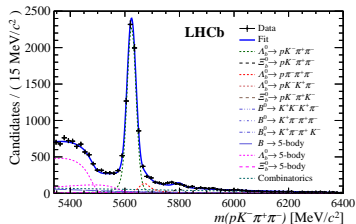
$$\Lambda_b^0 \rightarrow N(1520)^0 \rho^0$$


 \bar{X}_b


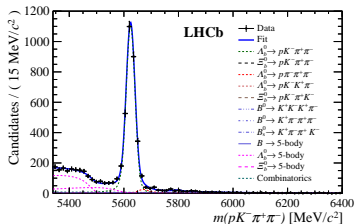
Fit projections

 X_b

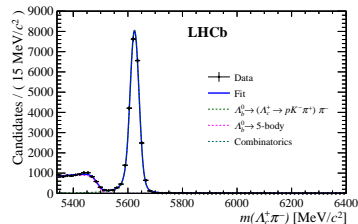
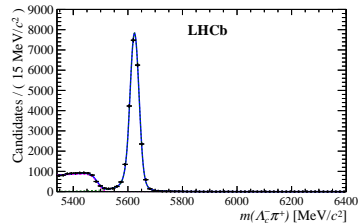
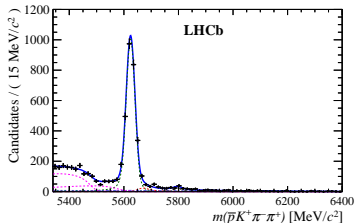
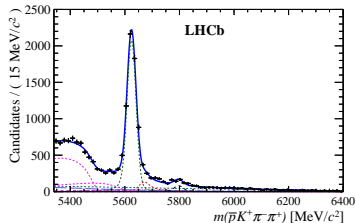
$$\Lambda_b^0/\Xi_b^0 \rightarrow pK^-\pi^+\pi^-$$



$$\Lambda_b^0 \rightarrow pK^-\pi^+\pi^- \text{ low mass}$$

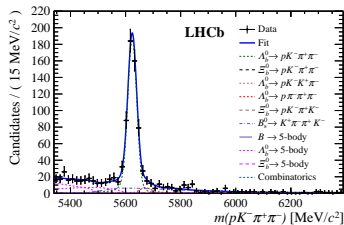


$$\Lambda_b^0 \rightarrow (\Lambda_c^+ \rightarrow pK^-\pi^+)\pi^-$$

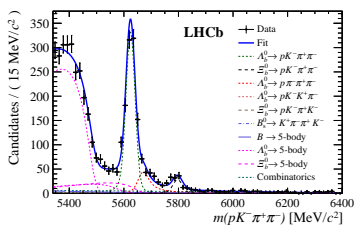
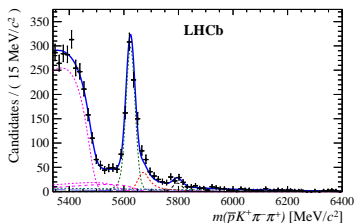
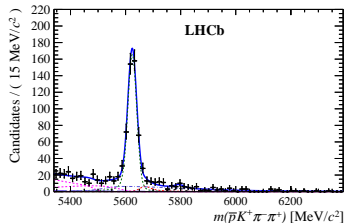
 \bar{X}_b 

Fit projections

$$\Lambda_b^0 \rightarrow p K_1(1410)^-$$

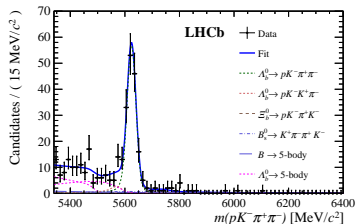
 X_b


$$\Lambda_b^0 \rightarrow \Delta(1232)^{++} K^- \pi^-$$

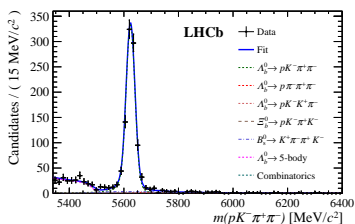
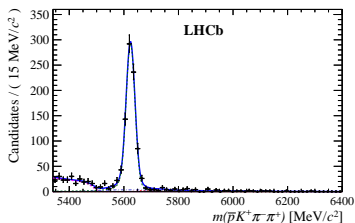
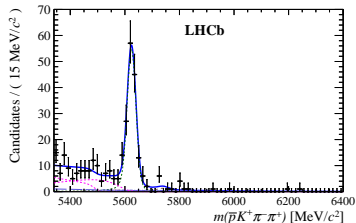

 \bar{X}_b


Fit projections

$$\Lambda_b^0 \rightarrow \Lambda(1520)\rho^0$$

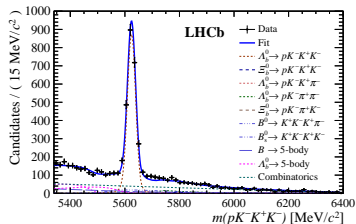
 X_b


$$\Lambda_b^0 \rightarrow N(1520)^0 K^{*0}$$

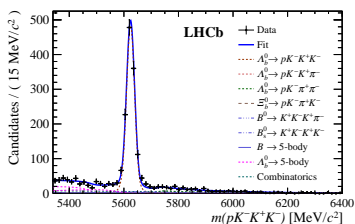
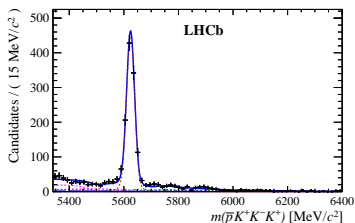
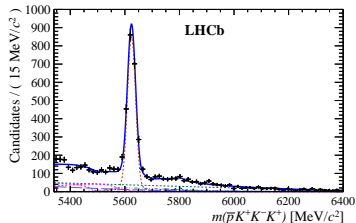

 \bar{X}_b


Fit projections

$$\Lambda_b^0 \rightarrow pK^-K^+K^-$$

 X_b


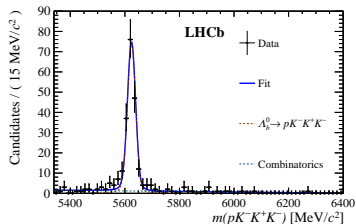
$$\Lambda_b^0 \rightarrow pK^-K^+K^- \text{ low mass}$$


 \bar{X}_b


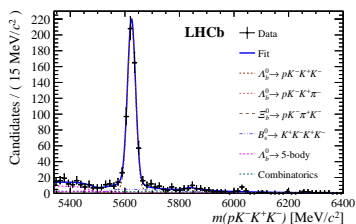
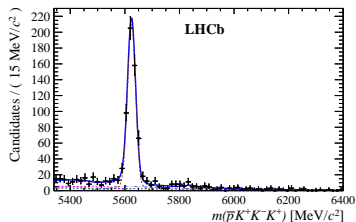
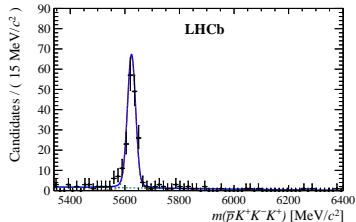
Fit projections

 X_b

$$\Lambda_b^0 \rightarrow \Lambda(1520)\phi$$



$$\Lambda_b^0 \rightarrow (pK^-)_{\text{high-mass}}\phi$$

 \bar{X}_b 

Systematics

Tracking detection efficiency

- Quantified separately for kaons (σ_K) and protons (σ_p)

Trigger efficiency (σ_{L0})

- Difference in hardware-level (L0) trigger efficiency between oppositely-charged hadrons

Production asymmetry (σ_{A_p})

- Difference in decay kinematics of signal and control channels \rightarrow incomplete cancellation
- Estimated from measurement of Λ_b^0 production asymmetry as a function of p_T and η ([Phys. Lett. B 774 \(2017\) 139](#))

PID calibration (σ_{PID})

- Finite size of calibration samples

Systematics

Decay mode	Absolute uncertainties (%)					Total (%)
	σ_K	σ_p	σ_{L0}	σ_{PID}	σ_{A_p}	
$\Lambda_b^0 \rightarrow p\pi^-\pi^+\pi^-$	—	0.20	0.06	0.42	0.28	0.54
$\Lambda_b^0 \rightarrow p\pi^-\pi^+\pi^-$ low mass	—	0.16	0.06	0.36	0.28	0.49
$\Lambda_b^0 \rightarrow pa_1(1260)^-$	—	0.20	0.09	0.48	0.28	0.60
$\Lambda_b^0 \rightarrow N(1520)^0\rho^0$	—	0.12	0.05	0.23	0.28	0.39
$\Lambda_b^0 \rightarrow \Delta(1232)^{++}\pi^-\pi^-$	—	0.18	0.05	0.47	0.28	0.59

Systematics

Decay mode	Absolute uncertainties (%)					Total (%)
	σ_K	σ_p	σ_{L0}	σ_{PID}	σ_{A_p}	
$\Lambda_b^0 \rightarrow pK^-\pi^+\pi^-$	0.17	0.20	0.06	0.41	0.24	0.55
$\Lambda_b^0 \rightarrow pK^-\pi^+\pi^-$ low mass	0.17	0.17	0.05	0.34	0.24	0.48
$\Lambda_b^0 \rightarrow \Lambda(1520)\rho^0$	0.12	0.12	0.04	0.36	0.24	0.49
$\Lambda_b^0 \rightarrow \Delta(1232)^{++}K^-\pi^-$	0.22	0.19	0.05	0.48	0.24	0.61
$\Lambda_b^0 \rightarrow N(1520)^0K^{*0}$	0.16	0.14	0.04	0.32	0.24	0.45
$\Lambda_b^0 \rightarrow pK_1(1410)^-$	0.16	0.14	0.11	0.58	0.24	0.74

Systematics

Decay mode	Absolute uncertainties (%)					Total (%)
	σ_K	σ_p	σ_{L0}	σ_{PID}	σ_{A_P}	
$\Lambda_b^0 \rightarrow pK^-K^+\pi^-$	—	0.21	0.06	0.40	0.55	0.72
$\Lambda_b^0 \rightarrow pK^-K^+K^-$	0.15	0.20	0.07	0.41	0.33	0.59
$\Lambda_b^0 \rightarrow pK^-K^+K^-$ low mass	0.16	0.17	0.05	0.37	0.33	0.55
$\Lambda_b^0 \rightarrow \Lambda(1520)\phi$	0.11	0.10	0.05	0.30	0.33	0.34
$\Lambda_b^0 \rightarrow (pK^-)_{\text{high-mass}}\phi$	0.15	0.14	0.06	0.58	0.33	0.64
$\Xi_b^0 \rightarrow pK^-\pi^+\pi^-$	0.17	0.20	0.05	0.42	0.24	0.55
$\Xi_b^0 \rightarrow pK^-\pi^+K^-$	0.15	0.20	0.05	0.41	0.55	0.73

Results

$$\Delta\mathcal{A}^{CP}(\Lambda_b^0 \rightarrow p\pi^-\pi^+\pi^-) = (+1.1 \pm 2.5 \pm 0.6) \%$$

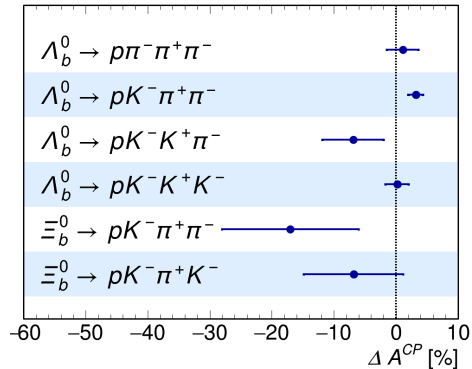
$$\Delta\mathcal{A}^{CP}(\Lambda_b^0 \rightarrow pK^-\pi^+\pi^-) = (+3.2 \pm 1.1 \pm 0.6) \%$$

$$\Delta\mathcal{A}^{CP}(\Lambda_b^0 \rightarrow pK^-K^+\pi^-) = (-6.9 \pm 4.9 \pm 0.8) \%$$

$$\Delta\mathcal{A}^{CP}(\Lambda_b^0 \rightarrow pK^-K^+K^-) = (+0.2 \pm 1.8 \pm 0.6) \%$$

$$\Delta\mathcal{A}^{CP}(\Xi_b^0 \rightarrow pK^-\pi^+\pi^-) = (-17 \pm 11 \pm 1) \%$$

$$\Delta\mathcal{A}^{CP}(\Xi_b^0 \rightarrow pK^-\pi^+K^-) = (-6.8 \pm 8.0 \pm 0.8) \%$$



Results

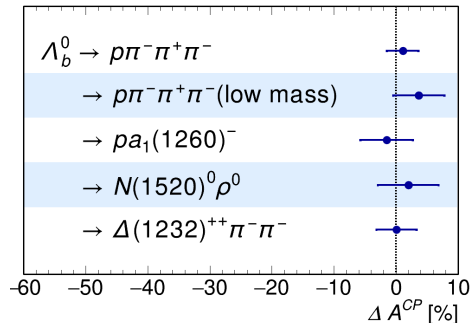
$$\Delta\mathcal{A}^{CP}(\Lambda_b^0 \rightarrow p\pi^-\pi^+\pi^-) = (+1.1 \pm 2.5 \pm 0.6) \%$$

$$\Delta\mathcal{A}^{CP}(\Lambda_b^0 \rightarrow p\pi^-\pi^+\pi^-)_{\text{low mass}} = (+3.7 \pm 4.1 \pm 0.5) \%$$

$$\Delta\mathcal{A}^{CP}(\Lambda_b^0 \rightarrow pa_1(1260)^-) = (-1.5 \pm 4.2 \pm 0.6) \%$$

$$\Delta\mathcal{A}^{CP}(\Lambda_b^0 \rightarrow N(1520)^0\rho^0) = (+2.0 \pm 4.9 \pm 0.4) \%$$

$$\Delta\mathcal{A}^{CP}(\Lambda_b^0 \rightarrow \Delta(1232)^{++}\pi^-\pi^-) = (+0.1 \pm 3.2 \pm 0.6) \%$$



Results

$$\Delta\mathcal{A}^{CP}(\Lambda_b^0 \rightarrow pK^-\pi^+\pi^-) = (+3.2 \pm 1.1 \pm 0.6) \%$$

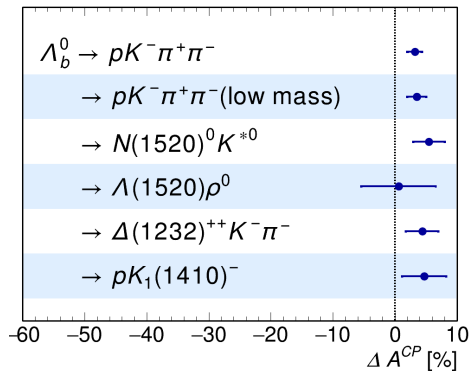
$$\Delta\mathcal{A}^{CP}(\Lambda_b^0 \rightarrow pK^-\pi^+\pi^-)_{\text{low mass}} = (+3.5 \pm 1.5 \pm 0.5) \%$$

$$\Delta\mathcal{A}^{CP}(\Lambda_b^0 \rightarrow N(1520)^0 K^{*0}) = (+5.5 \pm 2.5 \pm 0.5) \%$$

$$\Delta\mathcal{A}^{CP}(\Lambda_b^0 \rightarrow \Lambda(1520)\rho^0) = (+0.6 \pm 6.0 \pm 0.5) \%$$

$$\Delta\mathcal{A}^{CP}(\Lambda_b^0 \rightarrow \Delta(1232)^{++} K^-\pi^-) = (+4.4 \pm 2.6 \pm 0.6) \%$$

$$\Delta\mathcal{A}^{CP}(\Lambda_b^0 \rightarrow pK_1(1410)^-) = (+4.7 \pm 3.5 \pm 0.8) \%$$



Results

$$\Delta\mathcal{A}^{CP}(\Lambda_b^0 \rightarrow pK^-K^+K^-) = (+0.2 \pm 1.8 \pm 0.6) \%$$

$$\Delta\mathcal{A}^{CP}(\Lambda_b^0 \rightarrow pK^-K^+K^-)_{\text{low mass}} = (+2.7 \pm 2.3 \pm 0.6) \%$$

$$\Delta\mathcal{A}^{CP}(\Lambda_b^0 \rightarrow \Lambda(1520)\phi) = (+4.3 \pm 5.6 \pm 0.4) \%$$

$$\Delta\mathcal{A}^{CP}(\Lambda_b^0 \rightarrow (pK^-)_{\text{high-mass}}\phi) = (-0.7 \pm 3.3 \pm 0.7) \%$$

